SNX27-FERM-SNX1 complex structure rationalizes divergent trafficking pathways by SNX17 and SNX27

Xin Yong [1, 6] , Lin Zhao[1,6], Wenfeng Hu[1,6], Qingxiang Sun[2,6], Hyoungjun Ham[3,6], Zhe Liu[1,6], Jie Ren[4], Zhen Zhang[1], Yifei Zhou[1], Qin Yang[1], Xianming Mo[5], Junjie Hu[4], Daniel D. Billadeau[3*], Da Jia[1*]

Inventory of the SI appendix

Supplementary Methods

Molecular cloning

All plasmids used in this study are summarized in table S4. The gene encoding the human SNX27b FERM domain (residues 273-C) followed by a six amino acid linker (GGSGGS) and SNX1 residues 78-90 (SNX27-FERM-SNX1$^{78-90}$), human Very low-density lipoprotein receptor VLDLR (residues 820-C) and human amyloid precursor protein APP (residues 754-766) were synthesized, and cloned into the pGEX4T-1 vector. The genes encoding full-length SNX27, SNX1, SNX2, SNX17 were cloned into multiple vectors, including mCherryN1, pCDNA3.1^{+}, pMAL, or pET15b, for expression in mammalian cells or bacteria. Mutagenesis of plasmids used in this study were generated through site-directed PCR.

Protein expression and purification

The SNX27-FERM-SNX1$^{78-90}$ chimera construct was transformed into BL21(DE3) cells for protein expression. Expression of protein was induced by the addition of 0.5 mM isopropyl-β-d-thiogalactopyranoside (IPTG) until the cultured cells reached a density of OD_{600}~0.8-1.0 (1). After induction, cells were further grown at 18 °C for 16 h. The protein was first purified using Glutathione Sepharose 4B beads (GE), followed by on-column TEV protease cleavage. The eluted protein was further purified by ion-exchange and size-exclusion chromatography. The purified protein was stored in buffer (50 mM Tris, pH 8.0, 100 mM NaCl, 5% glycerol and 1 mM DTT), concentrated to 10 mg/mL, and used for crystallization. The seleno-methionine (SeMet) substituted chimera protein was purified similarly.

GST-tagged SNX27 FERM, SNX17 full-length, SNX1 and SNX2 were expressed and purified similar to the above chimera constructs. GST-tagged VLDLR and APP were expressed at 37 ℃ for 3 h. The proteins were captured by GSH resin, and eluted with buffer (20 mM Tris, pH 8.0, 200 mM NaCl, 1 mM DTT, 20mM GSH). Proteins were concentrated and stored at -80 ℃ for future use.

MBP-tagged SNX27 or SNX17 FERM domains were purified using Amylose Resin High Flow (NEB). The bound proteins were eluted using a buffer supplemented with 1% maltose, and dialyzed against buffer (50 mM Tris, pH 8.0 and 100 mM NaCl). His_6-tagged SNX27 FERM was captured by Ni-NTA resin (GE) and eluted with a buffer supplemented with 300 mM imidazole. Eluted protein was further purified using ion-exchange chromatography

Crystallization and Structural Determination of the SNX27-FERM-SNX1 complex

The SNX27-FERM-$SNX1^{78\text{-}90}$ chimera protein was crystallized by mixing the concentrated protein (10 mg/mL) with equal volume of reservoir buffer containing 4M HCOONa ($P6_1$ space group) or 0.12 M monosaccharides, 0.1 M buffer system3，pH8.5, 50%v/v Mix4 ($P2_12_12_1$). All crystals were cryo-protected using reservoir buffer supplemented with 20% glycerol, and were flash-frozen in liquid nitrogen. X-ray diffraction data was collected at Shanghai Synchrotron Radiation facility beamline BL17U1, and the phase was solved by Selenium Single-wavelength Anomalous Diffraction (Se-SAD). The resulting model was rebuilt with program Autobuild (2) and COOT (3), followed by repeated refinement with Refmac (4). The relevant data collection and refinement statistics are given in Table S1.

GST pull-down

GST pull-down experiments were performed as previously (5, 6). In Brief, 20 μg GST or GST-tagged proteins were mixed with Glutathione Sepharose 4B beads in a pull-down buffer (PB: 50 mM Tris, pH 8.0, 100 mM NaCl, 0.005% Triton-X100) for 2 h. Bait proteins (200 μg) were then added and incubated for another 30 min at 4˚C. The beads were then washed four times with 1 ml of PB. Bound proteins were visualized by Coomassie Blue staining or immunoblotting using respective antibodies.

Isothermal titration calorimetry

ITC experiments were performed on a Microcal iTC200 instrument at 16˚C, in an ITC buffer (50 mM Tris-Base pH 8.0, 100 mM NaCl) (7, 8). All proteins and peptides used for ITC assays were extensively dialyzed against the ITC buffer, and centrifuged at 15,000 rpm for 10 min prior to the experiment. The titration included one initial injection of 0.2 μL, followed by another 18 injections of 2 μL aliquots, with a spacing of 90s between injections.

To measure the SNX27-SNX1 interaction, approximately 1.5 mM of SNX1 peptide (residues 68-90) was titrated into approximately 50-70 μM of MBP-tagged SNX27-FERM. To measure the interactions with SNX17, 500-3000 μM of mouse P-selectin (residues 734–767), human LRP1 (residues 4497-4512), APP (residues 754-766), or APP-p were titrated into full-length SNX17 (50 μM). Experiments were triplicated and the data were analyzed using the Origin 7.0 software package (OriginLab) by fitting the “one set of sites” model.

Cell culture and transfection

Reagents for cell culture were obtained from Thermo Fisher unless stated otherwise. HeLa cells were maintained in high-glucose Dulbecco's modified Eagles medium (DMEM), supplemented with 10% (v/v) fetal bovine serum (FBS) and penicillin-streptomycin 1% (v/v) (Hyclone). Cells were grown under standard conditions and were transfected using LipoFiter™ 3.0 (Han bio) according to the manufacturer's protocol. For transfection, the plasmids were transfected with LipoFiter™ 3.0 (Han bio) according to the manufacturer's instructions.

Jurkat human CD4+ T cells and NALM6 B cells (both from ATCC) used in this study were cultured in RPMI 1640 media supplemented with final concentrations of 10% fetal bovine serum (FBS), 2 mM L-glutamine (Corning), 100 IU/mL penicillin, and 100 mg/mL streptomycin (both from Corning). Transfection assays were conducted using an BTX ECM 830 square-wave electroporator with a single pulse at 315 V for 10 ms. In each transfection, 8 million cells were transfected with 40 μg plasmid and the experiments were performed 2 days later.

Generation of SNX27-KO and SNX1+2 KO cell lines described previously (5). Briefly, cells were co-transfected by gRNA-encoding plasmid and a plasmid encoding GFP-tagged puromycin resistance. Two days after transfection, cells were subjected to puromycin selection. For siRNA-based knockdown, siRNA was transfected using RNAFit (Han bio).

Fluorescence microscopy and analysis

Immunofluorescence staining for HeLa cells was performed as previously described (5, 9). Cells

were first washed with PBS, fixed with 4% PFA, permeabilized with 0.1% Triton X-100, and blocked with 2% BSA in PBS. Cells were then incubated with indicated primary and secondary antibodies, sequentially. Images were acquired by Olympus FV-1000 confocal microscope and analyzed by NIH ImageJ software. All experiments were repeated at least three times.

Immunofluorescence for T cell – B cell conjugates were prepared as previously described (10). NALM6 B cells were stained with CellTracker Blue CMAC (7-amino-4-chloromethylcoumarin) according to manufacturer's instructions. Two million CMAC-labeled NALM6 B cells were then pulsed with or without 2 μg SEE (Toxin Technology, Inc.) in 1 ml serum-free (SF) RPMI at 37 ℃ for 30 min. Both B cells and Jurkat T cells were washed once with SF-RPMI, resuspended with SF-RPMI at 1 million cells/mL, and rested in a cell culture incubator (37 ℃, 5% CO2) for 10 min. Equal numbers of B cells and T cells were mixed and centrifuged together at 200 rpm for 5 min at 4 ℃ and incubated at 37 ℃ for 20 min. 120,000 cells were plated directly on poly-L-lysine-coated (0.1% in H2O (w/v); MilliporeSigma) 18 mm round coverslips (#1.5; Electron Microscopy Sciences), fixed with 4% paraformaldehyde (PFA) in PBS for 18 min, and permeabilized with 0.15% Triton-X 100 in PBS for 4 min at room temperature. Coverslips were stained with anti-VPS35 or anti-SNX1 antibodies, followed by donkey anti-goat IgG or donkey anti-rabbit IgG antibodies conjugated with Alexa Fluor (AF)-488 or AF-568. Polymerized F-actin was detected using AF-488- or AF-647-conjugated phalloidin. Coverslips were mounted on glass slides using Antifade mounting reagent. All confocal images were acquired on an Airyscan-equipped LSM800 confocal microscope with a 63x oil immersion objective of NA 1.4 (Zeiss). Images containing 10-15 conjugated T cells were taken for each experimental group, and

all experiments were independently repeated at least 3 times. Acquired raw images were processed with Airyscan on Zen Blue software (version 2.6; Zeiss) and exported to tiff format.

Colocalization analysis among YFP-SNX1, SNX27-mCherry, and VPS35 in conjugated T cells was performed and automated using a customized macro program within ImageJ (version 1.45s; NIH). A region of interest (ROI) was first defined as the area enclosed by SNX27-mCherry or YFP-SNX1 fluorescence. Pearson's correlation coefficient between two fluorescence channels within an ROI was then calculated using a Coloc2 plug-in within ImageJ with the Costes' automatic threshold setting (11).

Surface protein biotinylation assay

Surface protein biotinylation assay was performed as previously described (5, 9). Briefly, cells were transfected indicated plasmids. Cells from three 10-cm dishes were digested, washed, re-suspended, and incubated with Biotin reagent (Sulfo-NHS-SS-Biotin, Shanghai Sangon Co., Ltd) for 30 min at RT. Excessive biotin reagent was removed, and samples were washed with ice-cold PBS for three times. Cells were lysed in lysis buffer (50 mM Tris-Base pH 7.5, 50 mM NaCl, 0.5% NP40), and the supernatant was collected. Streptavidin agarose resin was mixed with the supernatant to capture biotinylated proteins. The resin was then washed 6 times with PBS, and the bound proteins were used for immunoblotting analysis.

Animals, Morpholino and mRNA injections

All zebrafish (Danio rerio) experiments were performed according to previous procedures (8, 12).

The following lines were used in this study: AB strain (wild-type), Tg[HuC:GFP] strain, and Tg[Hb9:GFP] strain. SNX27a (5'-CCGAGTTAAAGATGGCGGAGATCGA-3') and SNX27b (5'-AAATGGCAGATGTTGTCGAAGGAGA-3') morpholino oligonucleotide were purchased from GeneTools, and were used as previously described. At the one-cell stage, SNX27 MO (2.5ng) and/or mRNA (100ng) were injected into yolk or cells.

Whole-mount in situ hybridization (WISH)

Digoxigenin-UTP-labelled SNX27a antisense RNA probe was generated by *in vitro* transcription with Roche kit. WISH was performed according to previous procedures (8, 12). At 24 h post-fertilization, the zebrafish embryos were incubated with 10 mg/mL proteinase K at room temperature for 2 min, while samples at 48 hpf were incubated for 30 min, and then fixed with 4% paraformaldehyde. Then, the samples were then incubated with digoxigenin (DIG)-labeled antisense RNAs (SNX27a) at 65°C overnight. After removing the probes, the samples were incubated with alkaline Phosphatase (AP)-conjugated anti digoxigenin antibody (1:3000) at room temperature for 45 min. After washing, the samples were subjected to NBT/BCIP (Roche) staining according to the manufacturer's instructions.

Zebrafish total RNA extraction and RT-PCR

RNA isolation and RT-PCR for SNX27a RNA levels were carried out as previously published (8, 12). About 100 zebrafish embryos were collected for each sample. Total RNA was isolated using the RNeasy Micro Kit (Qiagen) and reverse transcribed using the Reverse-transcription PCR kit (TaKaRa DRR014A). PCR was performed using the appropriate primers.

Immunofluorescence staining of cryostat sections

Thick cryo-sections of zebrafish embryos (5-μm) were prepared using the cryo-microtome at -20℃. Immunofluorescence on cryo-sections was performed as previously described (8, 12). Briefly, samples were rehydrated in PBS, and blocked in PBS supplemented with 5% BSA. Samples were first incubated with primary antibody at 4℃ overnight, and washed with PBS for three times. Samples were then incubated with secondary antibody at room temperature for 1 h, followed by PBS wash and DAPI staining.

Statistical analysis

All statistical analyses of cell co-localization data were done in GraphPad Prism 8 using the statistical test indicated in the Figure Legends.

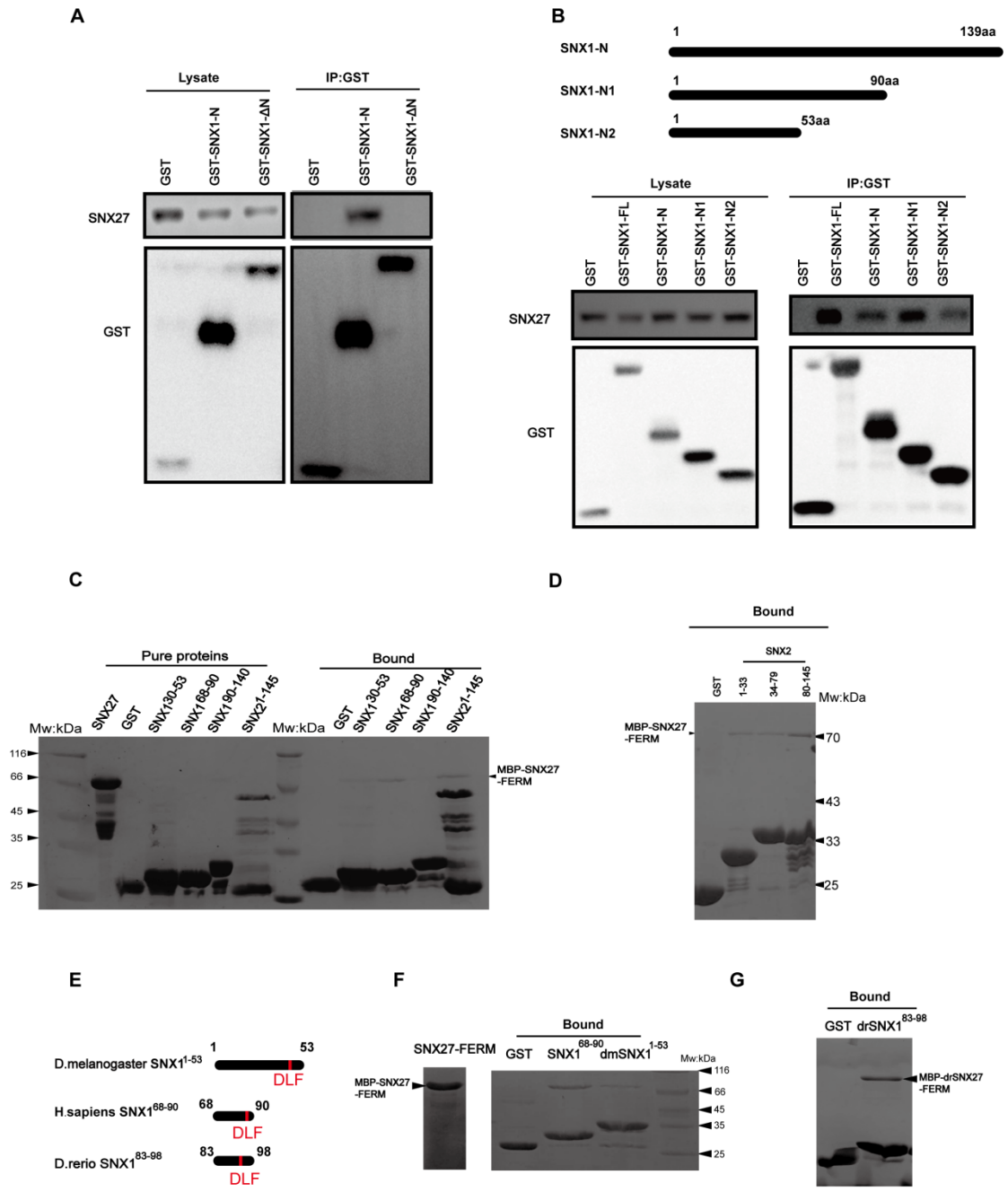

Figure S1. SNX1/2 bind to SNX27 FERM domain likely through the DLF motifs located at their N-terminus.

(A) HEK293T cells were transiently transfected with GST, GST tagged SNX1-N and SNX1-ΔN. GST tagged proteins were precipitated and endogenous SNX27 was detected by respective

antibody.

(B) Co-immunoprecipitation of GST or GST tagged SNX1 constructs transiently transfected in HEK293T cells.

(C) GST, GST-SNX1$^{30-53}$, GST-SNX1$^{68-90}$, GST-SNX1$^{90-140}$ and GST-SNX2$^{1-145}$ pull-down of purified MBP tagged SNX27-FERM. Shown is a Coomassie-stained gel of the purified proteins on the left and bound proteins on the right.

(D) GST tagged SNX2 constructs pull down purified MBP tagged SNX27-FERM. Shown is a Coomassie-stained gel of the bound proteins.

(E) A schematic diagram of *D.melanogaster* SNX1$^{1-53}$ and *H.sapiens* SNX1$^{68-90}$ and *D.rerio* SNX1$^{83-98}$ with DLF motif highlighted in red.

(F and G) SNX27 was tested for its binding ability toward indicated proteins shown in F and G. Shown are Coomassie-stained gels of the purified MBP-SNX27-FERM and bound proteins. SNX1$^{68-90}$: human SNX1; dmSNX1$^{1-53}$: *D. melanogaster* SNX1*;* drSNX1$^{83-98}$: *D.rerio* SNX1; drSNX27-FERM: *D.rerio* SNX27.

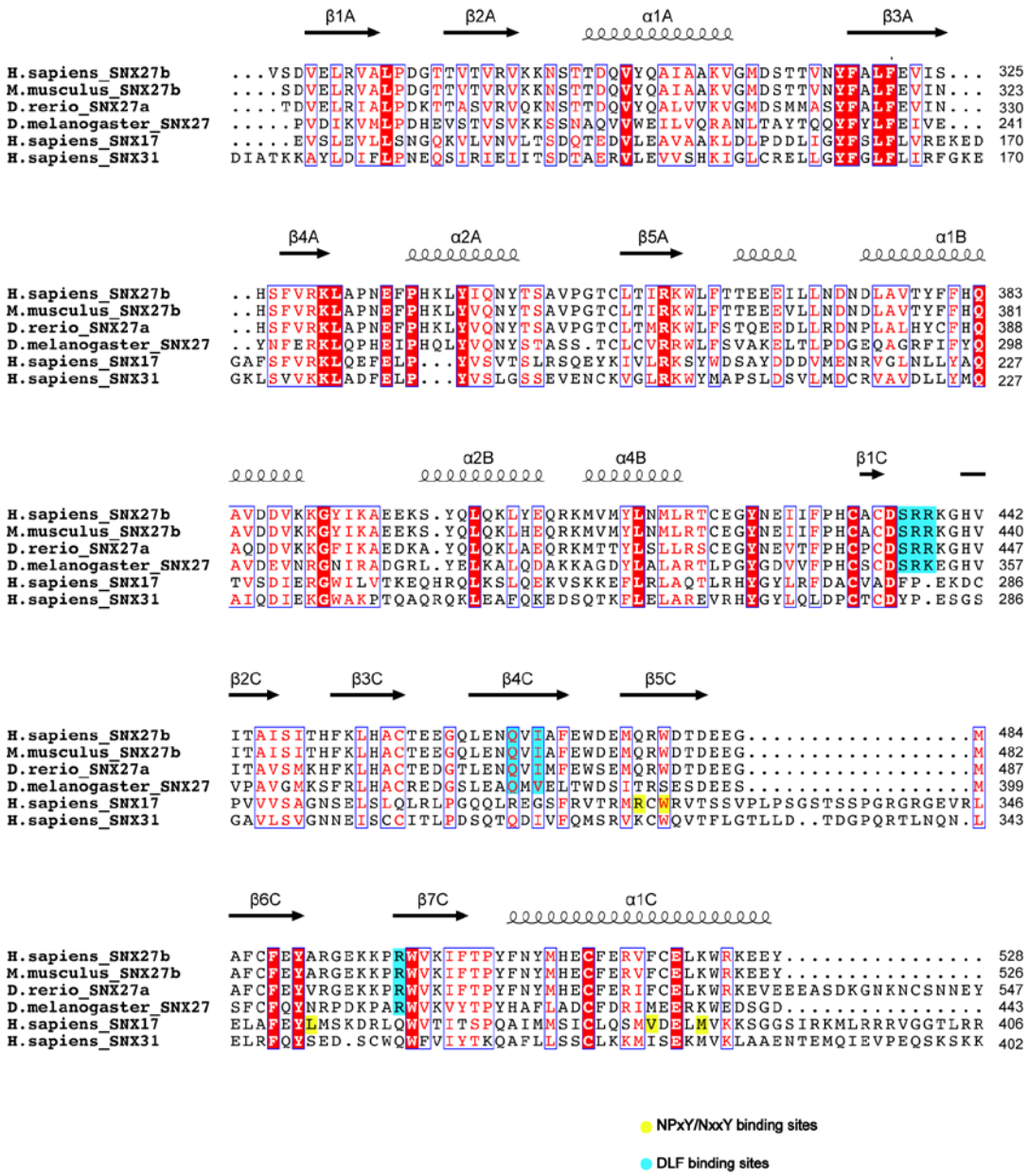

Figure S2. Sequence alignment of the FERM domains of SNX27, SNX17 and SNX31.

The listed secondary structure is derived from the crystal structure of the FERM domain of

SNX27 solved in this study. Residues contacting SNX1 peptide or critical for NPxY/NxxY binding are projected in cyan or yellow, respectively. The missing loop of SNX27 is located between β5C-β6C.

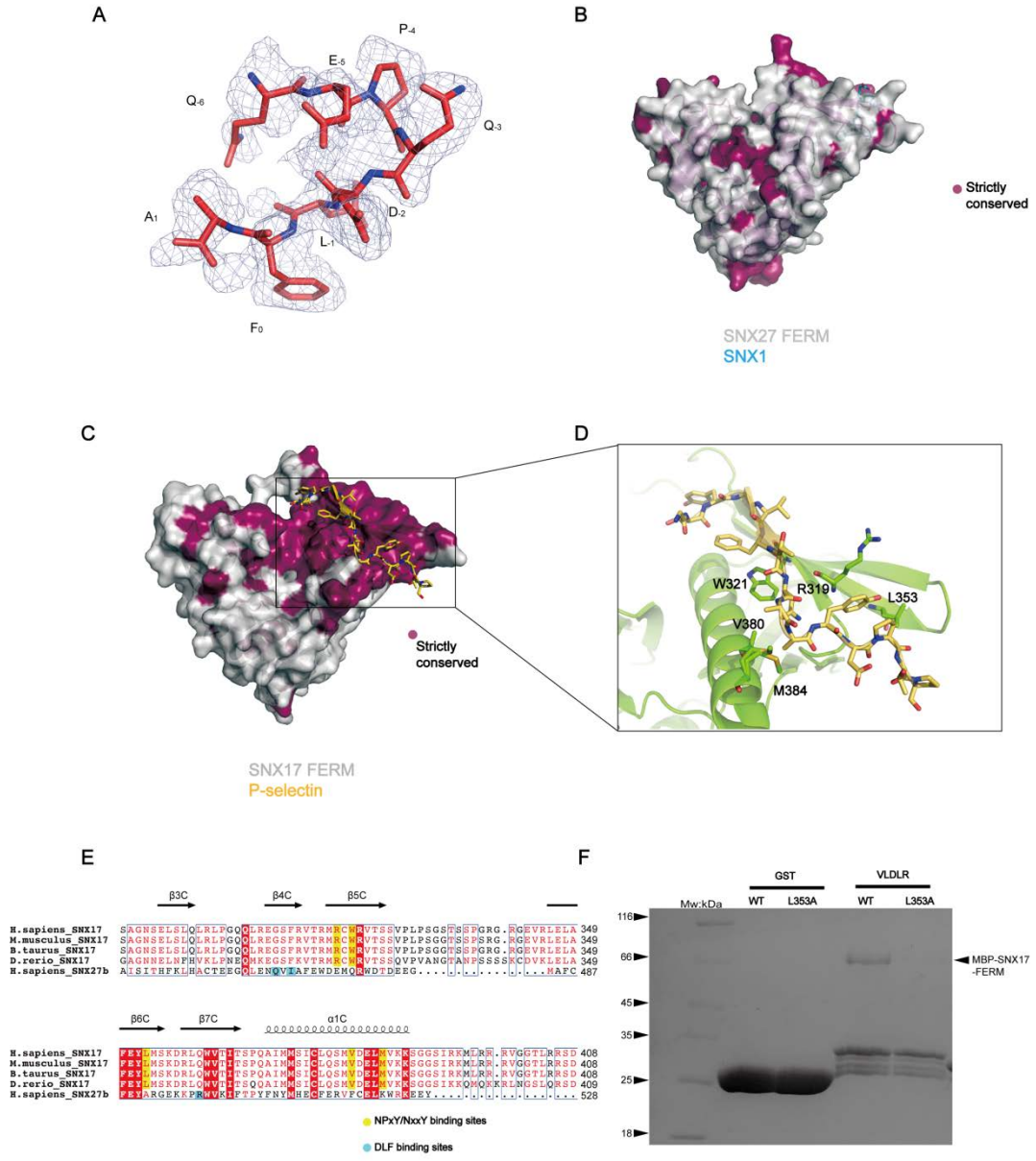

Figure S3. SNX27 FERM domain unlikely binds the NPxY/NxxY motif as SNX17.

(A) View of the Fo-Fc simulated-annealing omit map (gray) is contoured at a sigma level of 3σ, showing the refined SNX1 peptide structure in red sticks.

(B-C) Conservation analysis of the FERM domains of SNX27 and SNX17 using the ConSurf Server (https://consurf.tau.ac.il). The surfaces of both FERMs are colored as light gray (nonconserved) and purple (strictly conserved), with respective peptides shown in corresponding color. The NPxY/NxxY binding pocket is strictly conserved in SNX17, but not in SNX27. SNX17

and SNX27 are shown in the same orientations in (B) and (C). As the NPxY/NxxY motif and SNX1 bind to the distinct surfaces of SNX17 and SNX27, respectively, the SNX1 peptide is barely visible in (B).

(D) Close-up view of NPxY/NxxY binding pocket of SNX17-FERM, in which SNX17 is colored as green and P-selectin as yellow. SNX17 residues critical for NPxY/NxxY-cargo binding are highlighted.

(E) Sequence alignment of the NPxY/NxxY binding pocket of SNX17. SNX27 is included as a comparison. The listed secondary structure is obtained from PDB:4GXB. Residues critical for SNX1 or NPxY/NxxY binding are colored in cyan or yellow, respectively.

(F) GST, GST-VLDLR pull-down of purified MBP-SNX17-FERM WT and mutant. Shown is a Coomassie-stained gel of bound proteins.

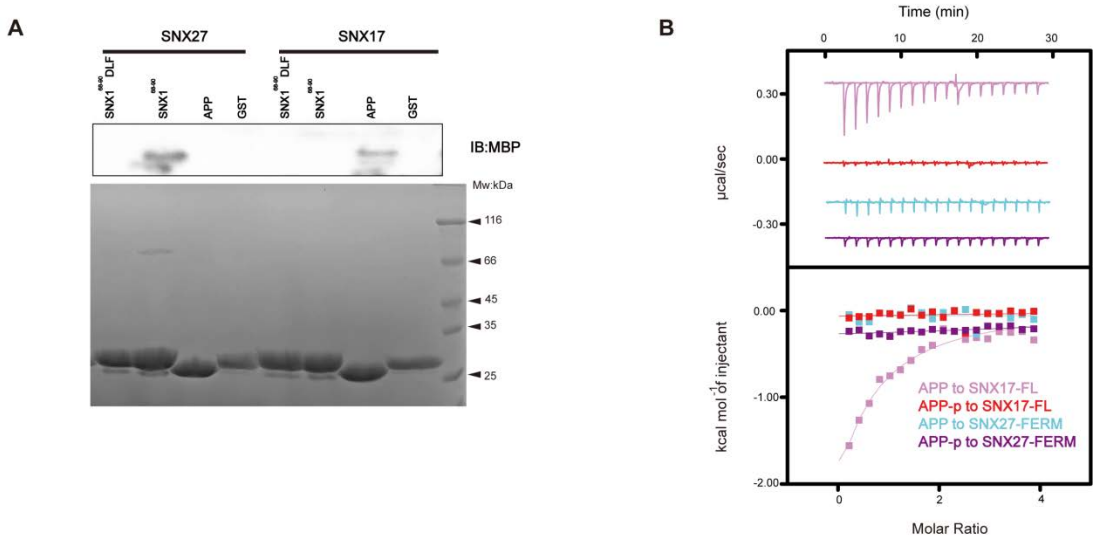

Figure S4. APP specifically interacts with the FERM domain of SNX17, but not SNX27.

(A) GST, GST-APP, GST-SNX1$^{68\text{-}90}$ and GST-SNX1$^{68\text{-}90}$DLF pull-down of purified MBP-SNX17-FERM or MBP-SNX27-FERM, respectively. Upper panel shows the bound proteins detected by immunoblot; lower panel shows a Coomassie-stained gel of bound proteins.

(B) Isothermal titration calorimetry of APP and APP-p titrated into purified MBP-SNX27-FERM or SNX17-FL in a buffer containing 50 mM Tris-Base pH 8.0, 100 mM NaCl at 16˚C. Raw data are listed at the top and integrated normalized data are listed at the bottom. Colors indicate the peptides used in the assay. Three separate experiments were performed in triplicate. Representative data from one experiment is shown.

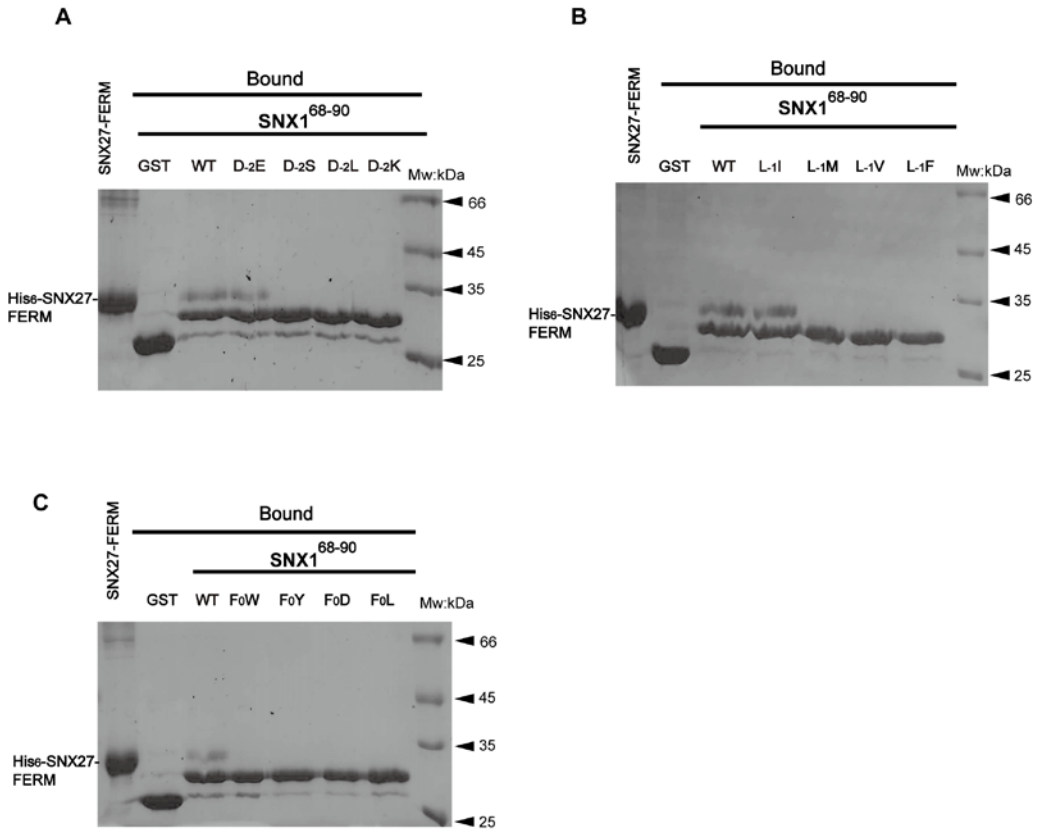

Figure S5. Systematic mutagenesis to identify the consensus sequence of the DLF motif.

(A-C) GST, GST-SNX1$^{68-90}$ WT and indicated mutants were subjected to a pull-down using purified His_6-SNX27-FERM. Shown are Coomassie blue-stained gels of GST bound proteins.

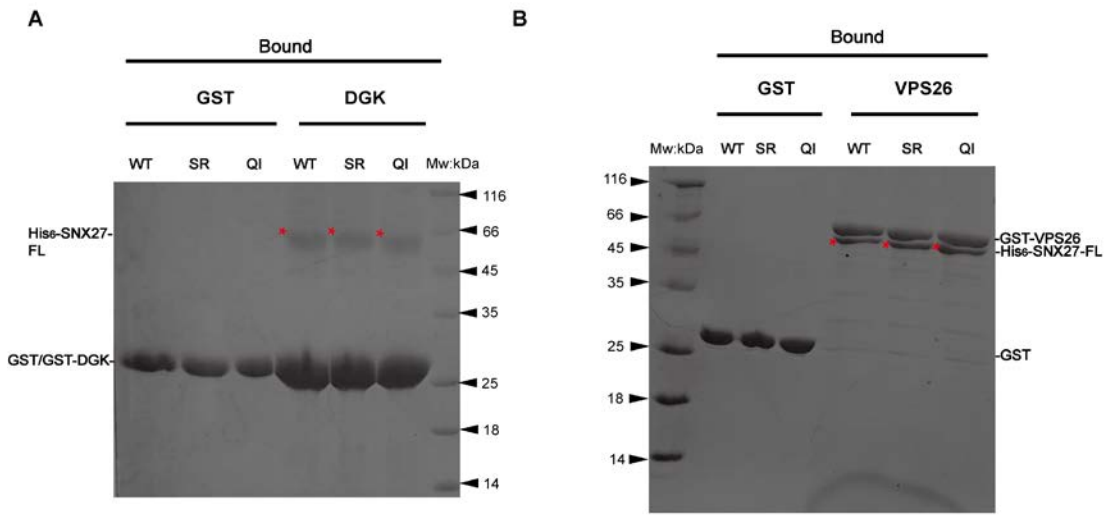

Figure S6. SNX27 associates with SNX1 and VPS26 or diacylglycerol kinase ζ (DGK) independently.

(A) GST or GST-DGK pull-down of purified full-length SNX27 WT, SR and QI mutants, separately. Shown is a coomassie-stained gel of bound proteins. * indicates the bound His_6-SNX27-FL.

(B) GST or GST-VPS26 pull-down of full-length SNX27 WT, SR and QI mutants, separately. Shown is a coomassie-stained gel of bound proteins. * indicates the bound His_6-SNX27-FL.

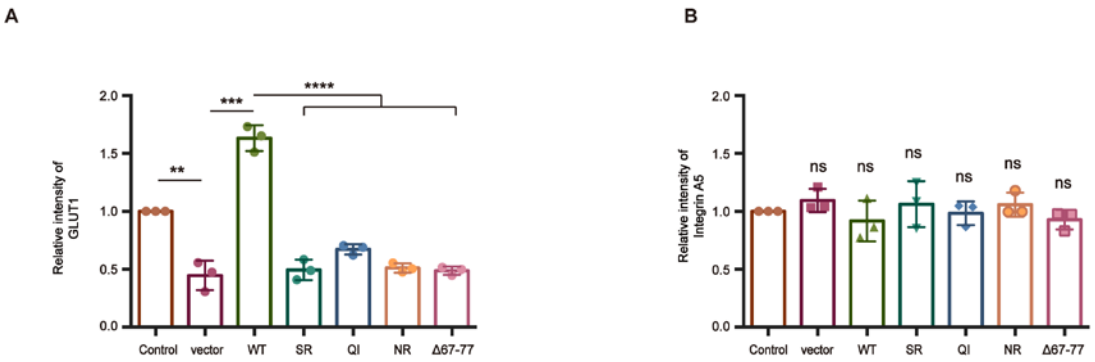

Figure S7. Quantitative analysis of GLUT1 and integrin A5.

(A) Band intensities of GLUT1 in Fig 5D were quantified with Image J and normalized to the control group (n = 3). Data are shown as mean ± SD and *P* values were calculated using t-test or one-way ANOVA, Tukey's multiple comparisons test. **P < 0.01, ***P < 0.001, 0.001<****P < 0.0001.

(B) Band intensities of integrin A5 in Fig 5D were quantified with Image J and normalized to the control group (n = 3). Data are shown as mean ± SD and *P* values were calculated using t-test or one-way ANOVA, Tukey's multiple comparisons test. Ns: not significant.

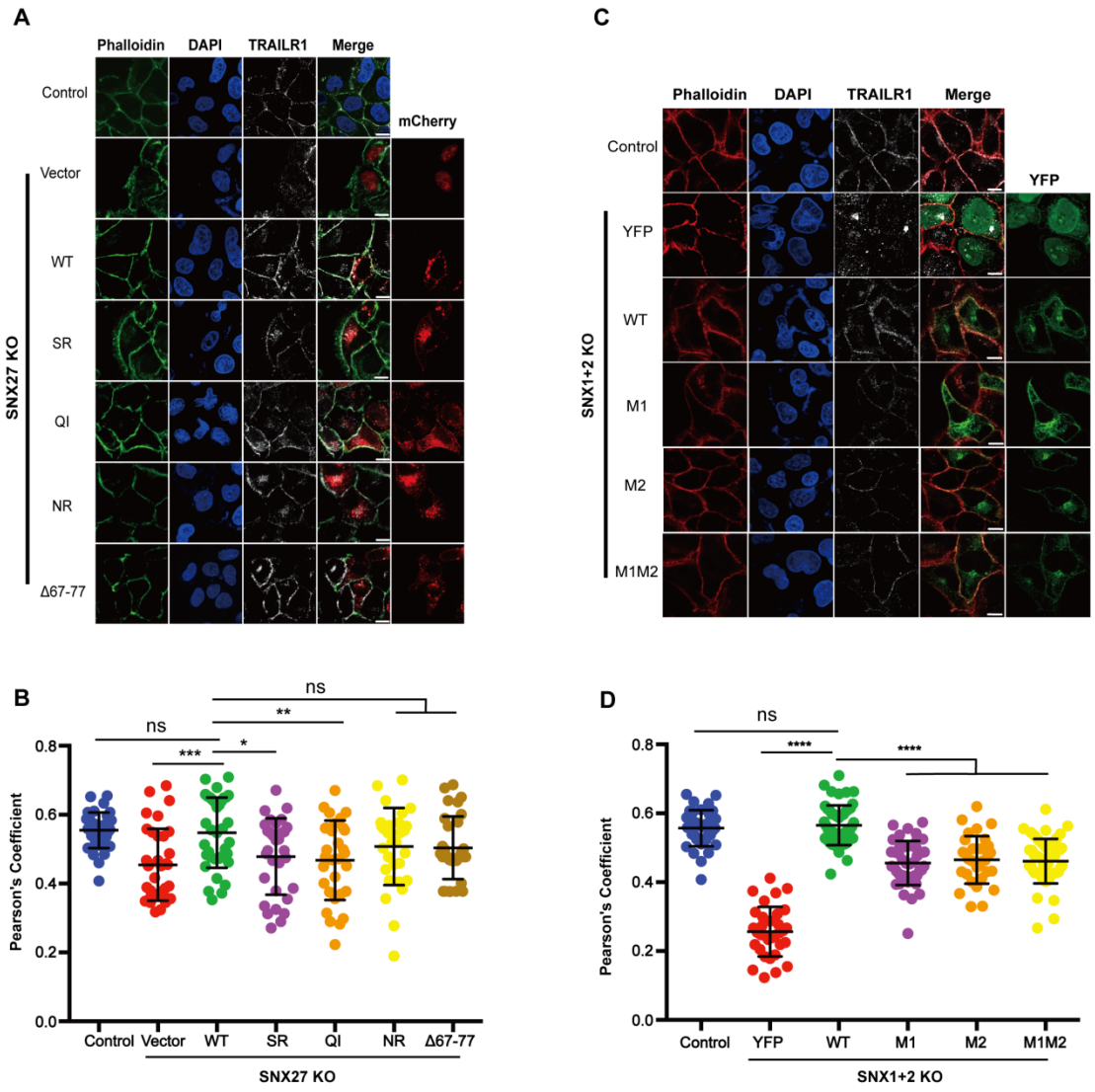

Figure S8. The interaction between SNX1 and SNX27 promotes TRAILR1 recycling.

(A) Surface distribution of TRAILR1 in SNX27 KO HeLa cell lines. The SNX27 KO cells were transfected with mCherry, mCherry-SNX27 WT, mCherry-SNX27 SR, mCherry-SNX27 QI, mCherry-SNX27 NR and mCherry-SNX27 Δ67-77 (left), while control cells were left untreated. Cells were then incubated with antibody against TRAILR1 (gray) and stained with phalloidin (green).

(B) Colocalization analysis between TRAILR1 and the F-actin marker phalloidin in A. Each dot represents Pearson's correlation coefficients from one cell. Data were presented as mean ± SD

and *P* values were calculated using one-way ANOVA, Tukey's multiple comparisons test. *P < 0.05, 0.05<**P < 0.01, ***P < 0.001, 0.001<****P < 0.0001, ns= not significant, figure is representative of n= 3 independent experiments with similar results.

(C) Surface distribution of TRAILR1 in SNX1+2 KO HeLa cell lines. The SNX1+2 KO cells were transfected with YFP, YFP-SNX1 WT, YFP-SNX1 M1, YFP-SNX1 M2 and YFP-SNX1 M1M2 (left), while control cells were left untreated. Cells were then incubated with antibody against TRAILR1 (gray) and stained with phalloidin (red).

(D) Colocalization analysis between TRAILR1 and the plasma membrane marker phalloidin in C. Each dot represents Pearson's correlation coefficients from one cell. Data were presented as mean ± SD and *P* values were calculated using one-way ANOVA, Tukey's multiple comparisons test. *P < 0.05, 0.05<**P < 0.01, ***P < 0.001, 0.001<****P < 0.0001, ns= not significant, figure is representative of n=3 independent experiments with similar results.

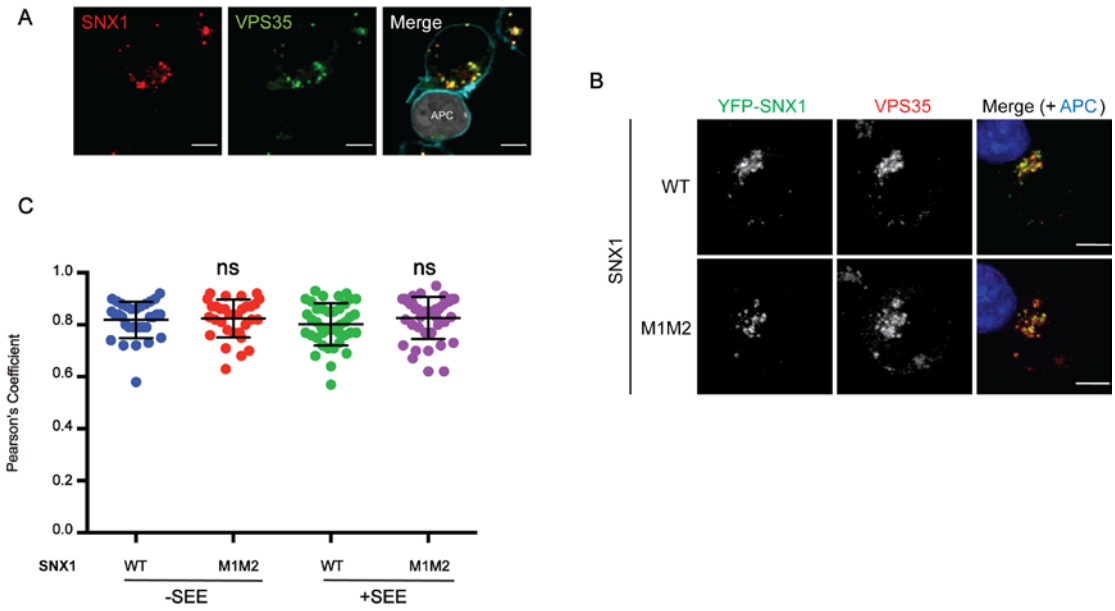

Figure S9. SNX1 is recruited to VPS35^{+} endosomes in Jurkat T cells, independent of its interaction with SNX27.

(A) Representative images showing endogenous SNX1 (red) localization in Jurkat T cells conjugated with SEE-pulsed NALM6 B cells (APC; gray). Cells were stained with indicated antibodies and F-actin was labeled with phalloidin (cyan).

(B-C) Jurkat T cells were transfected with plasmids expressing YFP tagged SNX1 WT or M1M2, and conjugated with NALM6 B cells. (B) Representative images showing localization of SNX1 (green) and endogenous VPS35 (red) in T cells conjugated with SEE-pulsed B cells (APC; blue). (C) Colocalization analysis between SNX1 and VPS35 within T cells conjugated with NALM6 B cells preloaded with or without SEE superantigen. Each dot represents a Pearson's correlation coefficient from a single conjugated T cell and error bars indicate SD. Statistical significance between WT and M1M2 mutant in each condition was determined using two-tailed unpaired t test, and none of the comparisons was significant. (A and B) Scale bar = 5 μm. Data shown are representative results from 3 independent experiments.

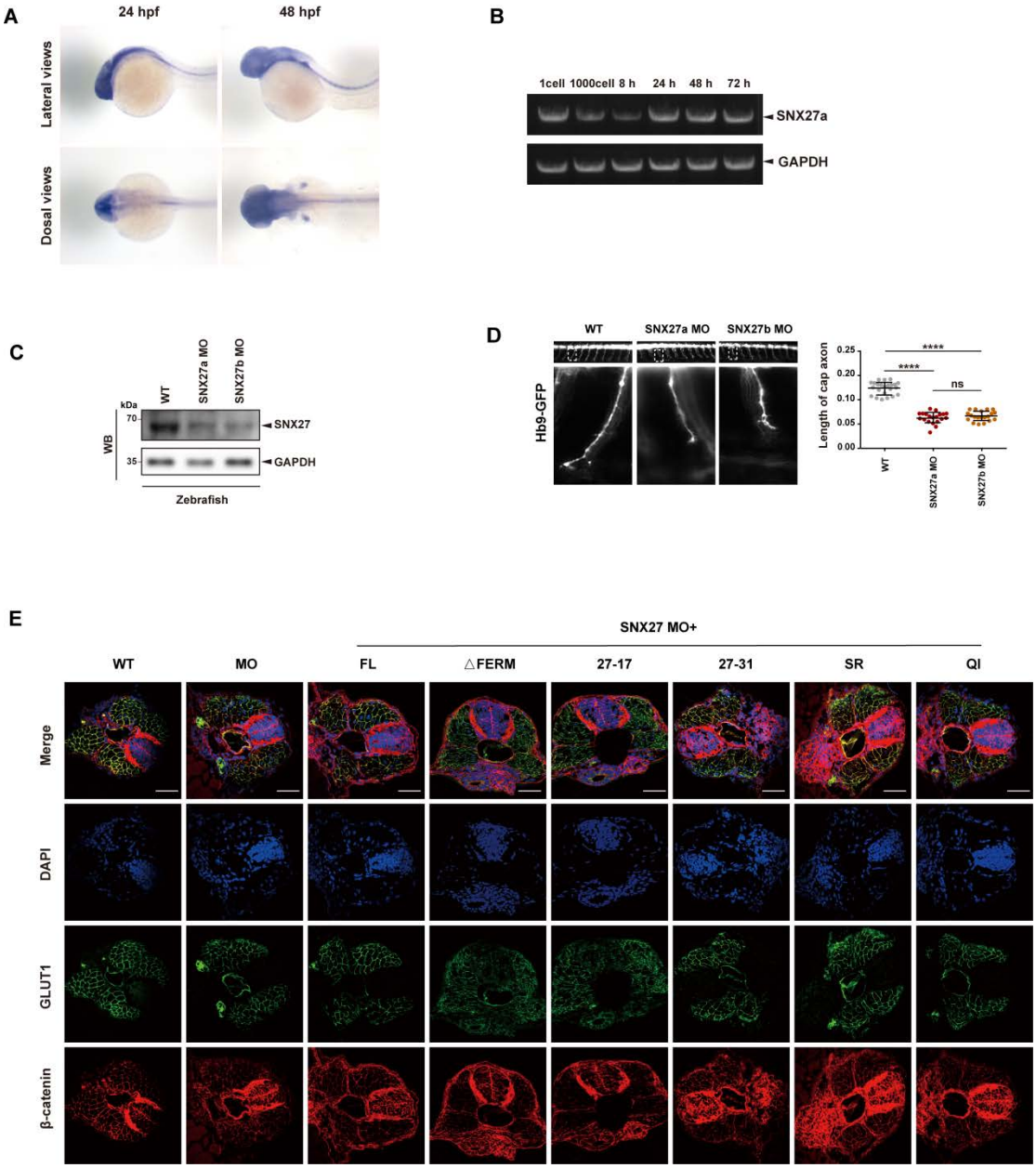

Fig S10. SNX27 functions in embryo development in zebrafish.

(A) The spatial expression of zebrafish SNX27 at 24 or 48 hpf determined by in situ hybridization is shown. Top: lateral views; Bottom: dorsal views.

(B) Semi-quantitative RT-PCR showing the relative expression level of SNX27a gene at different developmental stages. GAPDH was used as internal reference gene.

(C) Depletion of SNX27 by SNX27a or SNX27b MO was determined by immunoblotting using

anti-SNX27 antibody. GAPDH was used as internal reference gene. About 10 zebrafish embryos were collected for each sample. Representative images from one of two independent experiments are shown.

(D) Morphology of CaP axons from embryos at 30 hpf that were injected with SNX27a MO or SNX27b MO. All injections were performed at the one-cell stage of the Tg [hb9: GFP]ml2 transgenic zebrafish embryos. Lateral views (Top) and enlarged views (Bottom) of dashed squares are shown. Statistical results of the length of CaP axons in embryos. 25 axons from 5 embryos were used for analysis in control group (Con), while 20 axons from 4 embryos in SNX27a MO and SNX27b MO group. Data were shown as mean ± SD and *P* values were calculated using one-way ANOVA by Tukey's HSD test or t-test. ****P < 0.0001; ns= not significant.

(E)Transverse sections (close to yolk) of zebrafish embryos at 48 hpf were shown. GLUT1 (green) and β-catenin (red) were stained by respective antibodies, and representative images are shown. All injections were performed at one-cell stage of the development. Representative images of three independent experiments are shown. Scale bar: 50 μm.

Table S1. Data collection, phasing, and refinement statistics

	Se-Met	***Native***
Cell axial lengths (Å)	*a*=*b*=99.31, *c*=140.53;α=γ=90, β=120	*a*=43.19, *b*=72.94, *c*=104.00; α=β=γ=90
Spacegroup	$P6_1$	$P2_12_12_1$
Data collection		
Resolution range (Å)	86.01-3.26 (3.44-3.26)	59.72-1.95 (2.05-1.95)
Number of observed reflections	234635 (35868)	256090 (16959)
Number of unique reflections	12313 (1807)	24036 (3158)
Completeness (%)	100.0 (100.0)	96.8 (89.2)
Redundancy	19.1 (19.8)	10.7 (5.4)
R_{pim}	0.164 (0.730)	0.021 (0.239)
CC1/2	0.992 (0.726)	0.999 (0.926)
Mean I/I_{sigma}	12.1 (4.2)	23.8 (2.9)
Refinement		
Resolution range (Å)		22.27-1.95 (2.04-1.95)
Number of working reflections		22774 (3945)
Number of test reflections		2537 (126)
R_{work}[a]		0.171 (0.203)
R_{free}[b]		0.222 (0.250)
R.m.s. deviation bond lengths (Å)		0.008
R.m.s. deviation bond angles (°)		0.883
Average B-factors (Å2) (# of atoms)		46.4 (2353)
Ramachandran plot		
Allowed regions (%)		98.5
General allowed regions (%)		1.5
Disallowed regions (%)		0

R_{work}[a] = Σ|Fo – Fc|/|Fo|, where Fc and Fo are the calculated and observed structure factor amplitudes, respectively.

R_{free}[b] calculated as for R_{work} but for 5.0% of the total reflections chosen at random and omitted

from refinement for all data sets.

Table S2. Summary of Antibodies Used in this Study

Antibody	Source	Catalog#
GST	Santa Cruz	sc-138
DR4(TRAIL-RI)	CST	42533
GLUT1	Abcam	ab15309
SNX27	Abcam	ab77799
Integrinα5	Proteintech	10569-1-AP
GAPDH	Proteintech	10494-1-AP
mCherry	Proteintech	26765-1-AP
Goat anti-Rabbit IgG-HRP	Signalway Antibody(SAB)	L3012
Goat anti-Mouse IgG-HRP	Signalway Antibody(SAB)	L3032
TRITC AffiniPure Goat Anti-Mouse IgG (H+L)	Jackson ImmunoResearch	115-025-003
Alexa Fluor 647 AffiniPure Goat Anti-Rabbit IgG (H+L)	Jackson ImmunoResearch	111-605-003
Alexa Fluor 488 AffiniPure Goat Anti-Rabbit IgG (H+L)	Jackson ImmunoResearch	111-545-003
Donkey anti-Goat IgG (H+L) Secondary, Alexa Fluor Plus 488	Thermo Fisher	A32814TR
Donkey anti-Goat IgG (H+L) Secondary, Alexa Fluor 568	Thermo Fisher	A-11057
Donkey anti-Rabbit IgG (H+L) Secondary, Alexa Fluor 568	Thermo Fisher	A10042
MBP	Proteintech	15089-1-AP
VPS35	abcam	ab10099
SNX1	Proteintech	10304-1-AP

Table S3. Summary of Reagents in this Study

Reagents	Source	Catalog#
Phalloidin–Atto 532	Sigma	49429
Phalloidin–FITC	Sigma	E2888
Alexa Fluor™ 488 Phalloidin	Thermo Fisher	A12379
Alexa Fluor™ Plus 647 Phalloidin	Thermo Fisher	A30107
Phosphatase inhibitors	Bimake	B15001
Streptavidin Resin	Sangon Biotech	C006390
Sulfo-NHS-SS-Biotin	Sangon Biotech	C100216
RPMI 1640 Medium	Gibco	11875119
DMEM basic(1X)	Gibco	C11995500BT
Fetal Bovine Serum(FBS)	Gibco	
Penicillin–Streptomycin	Hyclone	SV30010
Penicillin-Streptomycin	Corning	30-002-CI
L-Glutamine	Corning	25-005-CI
Polyethylenimine (PEI)	Polysciences	24765-2
LipoFiter 3.0 Reagent	HanBio Technology	HB-TRLF3-1000
CellTracker™ Blue CMAC Dye	Thermo Fisher	C2110
SEE	Toxin Technology, Inc.	ET404
Poly-L-lysine hydrochloride	MilliporeSigma	P2658
18 mm round glass coverslips (#1.5)	Electron Microscopy Sciences	72290-08
16% Formaldehyde (w/v), Methanol-free	Thermo Fisher	28908
Triton™ X-100 Surfact-Amps™	Thermo Fisher	28314
Antifade Mountant	Thermo Fisher	P36961
RNAFit	HanBio Technology	HB-RF3-1000
Bovine Serum Albumin (BSA)	BioFroXX	4242GR100
0.25% Trypsin-EDTA(1X)	Gibco	25200-072
PVDF transfer membranes	Millipore	ISEQ00010
chemiluminescent HRP substrate	Millipore	WBKLS0500
lysis buffer	Beyotime	P0013

Table S4. Summary of DNA constructs used in this Study

Construct name	Description	Source or reference
	SNX1	
YFP-SNX1	HA-YFP-SNX1-WT	(Jia et al.,2016)
YFP-SNX1-N	HA-YFP-SNX1 (residues 1-140)	This study
YFP-SNX1-M1	HA-YFP-SNX1 (residues 1-140) $_{45}$DIF$_{47}$/AAA	This study
YFP-SNX1-M2	HA-YFP-SNX1 (residues 1-140) $_{87}$DLF$_{89}$/AAA	This study
YFP-SNX1-M1M2	HA-YFP-SNX1 (residues 1-140)$_{45}$DIF$_{47}$/AAA&$_{87}$DLF$_{89}$/AAA	This study
GST-SNX1	PEBG-GST-SNX1 full length	This study
GST-SNX1-N	PEBG-GST-SNX1 (residues 1-140)	This study
GST-SNX1-ΔN	PEBG-GST- SNX1 (residues 141-C)	This study
MBP-SNX1-ΔN	pMAL-SNX1 (residues 141-C)	This study
MBP-SNX1-N	pMAL-SNX1 (residues 1-140)	This study
GST-SNX1 30-53	pGEX4T1-SNX1 (residues 30-53)	This study
GST-SNX1 68-90	pGEX4T1-SNX1 (residues 68-90)	This study
GST-SNX1 90-140	pGEX4T1-SNX1 (residues 90-140)	This study
GST-dmSNX1 1-53	pGEX4T1-D.melangogaster SNX1 (residues 1-53)	This study
GST-drSNX1 83-98	pGEX4T1-D.rerio SNX1 (residues 83-98)	This study
GST-SNX1 68-90 E$_{-5}$A	pGEX4T1-SNX1 (residues 68-90) E84A	This study
GST-SNX1 68-90 Q$_{-3}$A	pGEX4T1-SNX1 (residues 68-90) Q86A	This study
GST-SNX1 68-90 D$_{-2}$A	pGEX4T1-SNX1 (residues 68-90) D87A	This study
GST-SNX1 68-90 L$_{-1}$A	pGEX4T1-SNX1 (residues 68-90) L88A	This study
GST-SNX1 68-90 F$_{0}$A	pGEX4T1-SNX1 (residues 68-90) F89A	This study
GST-SNX1 68-90 DLF	pGEX4T1-SNX1 (residues 68-90) $_{-2}$DLF$_{0}$/AAA	This study
	SNX27	
mCherry-SNX27	pmCherryN1-SNX27 full length	This study
mCherry-SNX27 SR	pmCherryN1-SNX27S436R437/AA	This study
mCherry-SNX27 QI	pmCherryN1-SNX27 Q465I467/AA	This study

mCherry-SNX27 NR	pmCherryN1-SNX27 N56R58/AA	This study
mCherry-SNX27 Δ67-77	pmCherryN1-SNX27 Δ67-77	This study
His_6-SNX27-FL	pET15b-SNX27 full length	This study
His_6-SNX27-FL SR	pET15b-SNX27 S436R437/AA	This study
His_6-SNX27-FL QI	pET15b-SNX27 Q465I467/AA	This study
GST-SNX27	pEBB-GST-SNX27 full length	This study
GST-SNX27-FERM	pGEX4T1-SNX27 (residues 273-C)	This study
GST-SNX27-FERM/SNX1 68-90	pGEX4T1-SNX27 (residues 273-C) linked to C-terminal SNX1 (residues 68-90)	This study
MBP-SNX27-FERM	pMAL-SNX27 (residues 273-C)	This study
MBP-drSNX27-FERM	pMAL-D.rerio SNX27（residues 276-547）	This study
MBP-SNX27-FERM SR	pMAL-SNX27 (residues 273-C) S436R437/AA	This study
MBP-SNX27-FERM R438A	pMAL-SNX27 (residues 273-C) R438A	This study
MBP-SNX27-FERM R438E	pMAL-SNX27 (residues 273-C) R438E	This study
MBP-SNX27-FERM QI	pMAL-SNX27 (residues 273-C) Q465I467/AA	This study
MBP-SNX27-FERM R498A	pMAL-SNX27 (residues 273-C) R498A	This study
His6-SNX27-FERM	pET15b-SNX27 (residues 273-C)	This study
SNX27 FL	pcDNA3.1 SNX27 full length	This study
SNX27 ΔFERM	pcDNA3.1 SNX27 (residues 1-273)	This study
SNX27 SR	pcDNA3.1 SNX27 S436R437/AA	This study
SNX27 QI	pcDNA3.1 SNX27 Q465I467/AA	This study
SNX27-17	pcDNA3.1 SNX27 (residues 1-273) fused to C-terminal SNX17 FERM (residues 110-386)	This study
SNX27-31	pcDNA3.1 SNX27 (residues 1-273) fused to C-terminal SNX31 FERM (residues 115-387)	
	SNX17	
GST-SNX17	pGEX4T1-SNX17 full length	This study
MBP-SNX17-FERM	pMAL-SNX17 (residues 110-386)	This study
MBP-SNX17-FERM L353A	pMAL-SNX17 (residues 110-386) L353A	This study
	SNX2	
GST-SNX2 1-145	pGEX4T1-SNX2 1-145	This study
GST-SNX2 1-33	pGEX4T1-SNX2 1-33	This study

GST-SNX2 34-79	pGEX4T1-SNX2 34-79	This study
GST-SNX2 80-145	pGEX4T1-SNX2 80-145	This study
	others	
GST-VLDLR	pGEX4T1-VLDLR (residues 820-C)	This study
GST-APP	pGEX4T1-APP (residues 754-766)	This study
GST-DGK	pGEX4T1-DGK-REDQETAV	This study
GST-VPS26	pGEX4T1-VPS26 (residues 9-C)	This study

References

1. Yong X*, et al.* (2018) Expression and purification of the SNX1/SNX6 complex. *Protein Expr Purif* 151:93-98.
2. Terwilliger TC*, et al.* (2008) Iterative model building, structure refinement and density modification with the PHENIX AutoBuild wizard. *Acta crystallographica. Section D, Biological crystallography* 64(Pt 1):61-69.
3. Emsley P, Lohkamp B, Scott WG, & Cowtan K (2010) Features and development of Coot. *Acta crystallographica. Section D, Biological crystallography* 66(Pt 4):486-501.
4. Murshudov GN, Vagin AA, & Dodson EJ (1997) Refinement of macromolecular structures by the maximum-likelihood method. *Acta crystallographica. Section D, Biological crystallography* 53(Pt 3):240-255.
5. Yong X*, et al.* (2020) Mechanism of cargo recognition by retromer-linked SNX-BAR proteins. *PLoS biology* 18(3):e3000631.
6. Jia D*, et al.* (2016) Structural and mechanistic insights into regulation of the retromer coat by TBC1d5. *Nat Commun* 7:13305.
7. Yao J*, et al.* (2018) Mechanism of inhibition of retromer transport by the bacterial effector RidL. *Proc Natl Acad Sci U S A* 115(7):E1446-E1454.
8. Qin J*, et al.* (2020) Structural and mechanistic insights into secretagogin-mediated exocytosis. *Proc Natl Acad Sci U S A* 117(12):6559-6570.
9. Singla A*, et al.* (2019) Endosomal PI(3)P regulation by the COMMD/CCDC22/CCDC93 (CCC) complex controls membrane protein recycling. *Nat Commun* 10(1):4271.
10. Nolz JC*, et al.* (2008) The WAVE2 complex regulates T cell receptor signaling to integrins via Abl- and CrkL-C3G-mediated activation of Rap1. *J Cell Biol* 182(6):1231-1244.
11. Costes SV*, et al.* (2004) Automatic and quantitative measurement of protein-protein colocalization in live cells. *Biophysical journal* 86(6):3993-4003.
12. Liu D*, et al.* (2020) Structure of TBC1D23 N-terminus reveals a novel role for rhodanese domain. *PLoS biology* 18(5):e3000746.